Radiative corrections for the correlator of $(0^{++}, 1^{-+})$ light hybrid currents

H.Y. Jin and J.G. Körner *

Institut für Physik, Johannes Gutenberg-Universität, Staudinger Weg 7, D 55099 Mainz , Germany

Abstract

We calculate the radiative corrections to the current-current correlator of the hybrid current $g\bar{q}(x)\gamma_\nu iG^a_{\mu\nu}T^a q(x)$. Based on this new result we use the QCD sum rule approach to estimate lower bounds on the masses of the $J^{PC}=1^{-+}$ and 0^{++} light hybrids.

1 Introduction

Mesons with exotic quantum number have attracted a great deal of attention in low energy strong interaction physics. They constitute another intrinsic construction of matter beyond the quark model in QCD. Although these mesons have not been confirmed yet, recent experiments indeed give some evidence for their possible existence. The E852 Collaboration at BNL has reported a $J^{PC} = 1^{-+}$ isovector resonance $\hat{\rho}(1405)$ in the reaction $\pi^- p \to \eta\pi^0 n$, with a mass of $1370 \pm 16^{+50}_{-30}$ MeV and a width of $385 \pm 40^{+65}_{-105}$ MeV [1]. This state appears to have been confirmed by the Crystal Barrel Collaboration in $p\bar{p}$ annihilation with a mass of $1400 \pm 20 \pm 20$ MeV and a width of $310 \pm 50^{+50}_{-30}$ MeV [2]. E852 lays claim to another $J^{pc} = 1^{-+}$ isovector state $\hat{\rho}(1600)$ in the reaction $\pi^- p \to \pi^+\pi^-\pi^- p$, with a mass and width of 1593 ± 8 MeV and 168 ± 20 MeV, resp., which decays into $\rho\pi$ [3]. We will have to wait for further confirmation of these states.

The mass values for the exotic 1^{-+} state reported by the different experiments disagree with most theoretical predictions. The flux-tube model predicts the lowest-lying 1^{-+} hybrid meson to have a mass of 1.9 GeV [4], which is consistent with lattice QCD studies which predict the lightest exotic hybrid 1^{-+} to have a mass of 2.0 GeV [5]. Besides, the flux-tube model also predicts that the $b_1\pi$ and $f_1\pi$ modes dominate in 1^{-+} hybrid meson decay [6], in contradiction with the experiments in which the mode $\rho\pi$ is dominant. Differing from the flux-tube model predictions calculations based on the QCD sum rule (QCDSR) approach seem to be closer to experimental results [7]. The preliminary results of QCDSR show that the lightest exotic hybrid meson has a mass around 1.6 GeV and a dominant $\rho\pi$ decay mode [9]. This is consistent with the second 1^{-+} state claimed by E852. The discrepancies between

---

*jhy@thep.physik.uni-mainz.de, koerner@thep.physik.uni-mainz.de

the different model predictions may come from different sources. The flux-tube model uses a non-relativistic linear potential model, which is not so suitable for the light-mass system. On the other hand, many effects, such as higher order terms in the OPE and radiative corrections, may affect the QCDSR predictions. Further theoretical studies are obviously necessary.

In this paper, we calculate the radiative corrections to the current-current correlator of the hybrid current $\bar{q}(x)\gamma_\nu ig G^a_{\mu\nu}T^a q(x)$. Using this new result, we recalculate the masses of the 1^{-+} and 0^{++} hybrids via the standard QCDSR method. We find that, including the radiative corrections, QCDSR have less room to accommodate the recent experimental data.

2   Renormalization of the current $j_\mu = \bar{q}\gamma_\nu ig G^a_{\mu\nu}T^a q$

The operator-mixing problems associated with the renormalization of composite operators have been discussed sometimes ago [8]. For instance, a given gauge invariant operator can mix with other gauge invariant operators, with non-gauge invariant operators which vanish by equations of motion and with operators containing ghosts. The mixing operators must have the same CP quantum number and the same dimension as the original one. In our case, the complete set of operators which can mix with $\bar{q}\gamma_\nu ig G^a_{\mu\nu}T^a q$ is given by

$$
\begin{aligned}
j^1_\mu &= \bar{q}\gamma_\nu ig G_{\mu\nu}q, \\
j^2_\mu &= \bar{q}(\vec{D}_\mu \vec{\slashed{D}} - \overleftarrow{\slashed{D}}\overleftarrow{D}_\mu)q, \\
j^3_\mu &= \bar{q}(\gamma_\mu \sigma_{\alpha\beta}g G_{\alpha\beta} - g G_{\alpha\beta}\sigma_{\alpha\beta}\gamma_\mu)q, \\
j^4_\mu &= \bar{q}(\gamma_\mu \vec{\slashed{D}}\vec{\slashed{D}} - \overleftarrow{\slashed{D}}\overleftarrow{\slashed{D}}\gamma_\mu)q, \\
j^5_\mu &= \bar{q}(\gamma_\mu ig\slashed{A}\vec{\slashed{D}} + \overleftarrow{\slashed{D}}ig\slashed{A}\gamma_\mu)q, \\
j^6_\mu &= \bar{q}(ig A_\mu \vec{\slashed{D}} + \overleftarrow{\slashed{D}}ig A_\mu)q.
\end{aligned}
\tag{1}
$$

Note that there is no dimension-five operator containing ghost fields in the set (1). In (1) we have defined $\sigma_{\alpha\beta} = \frac{i}{2}[\gamma_\alpha, \gamma_\beta]$ and the covariant derivatives $\vec{D}_\mu = \vec{\partial}_\mu + ig A_\mu$, $\overleftarrow{D}_\mu = \overleftarrow{\partial}_\mu - ig A_\mu$, which act on right and left fields, respectively. The fields and couplings in (1) are bare. Only j^1_μ and j^3_μ are physical currents. The other currents correspond to so-called nuisance operators which vanish by the equations of motion.

Renormalizing the composite operator corresponding to j^1_μ we obtain

$$
[j^1_\mu] = Z_1 j^1_\mu + Z_2 j^2_\mu + Z_3 j^3_\mu + Z_4 j^4_\mu + Z_5 j^5_\mu + Z_6 j^6_\mu,
\tag{2}
$$

In order to determine the coefficients $Z_i (i = 1, 6)$, we insert the currents into 1PI diagrams and extract the ultraviolet divergences. We find that the divergences associated with the $\bar{q}qg$-vertex are sufficient to determine all counterterms. The relevant diagrams are shown in Fig.1. In Feynman gauge, we obtain

$$
Z_1 = 1 + \frac{113}{18}\frac{g^2}{16\pi^2}\frac{1}{\epsilon},
$$

$$Z_2 = -\frac{4}{9}\frac{g^2}{16\pi^2}\frac{1}{\epsilon},$$
$$Z_3 = -\frac{49}{72}\frac{g^2}{16\pi^2}\frac{1}{\epsilon},$$
$$Z_4 = -\frac{8}{9}\frac{g^2}{16\pi^2}\frac{1}{\epsilon}, \tag{3}$$
$$Z_5 = \frac{19}{72}\frac{g^2}{16\pi^2}\frac{1}{\epsilon},$$
$$Z_6 = \frac{35}{36}\frac{g^2}{16\pi^2}\frac{1}{\epsilon},$$

where we use dimensional regularization.

3 Next-to leading order correction to the current-current correlator

Let us consider the current-current correlator

$$\Pi_{\mu\nu}(q^2) = i\int d^4x e^{iqx}\langle 0|T\{j_\mu(x), j_\nu^+(0)\}|0\rangle \tag{4}$$
$$= (\frac{q_\mu q_\nu}{q^2} - g_{\mu\nu})\Pi_v(Q^2) + \frac{q_\mu q_\nu}{q^2}\Pi_s(q^2)$$

where $j_\mu(x) = \bar{u}(x)\gamma_\nu ig G_{\mu\nu}^a T^a u(x)$. The invariants $\Pi_v(Q^2)$ and $\Pi_s(Q^2)$ correspond to the contributions from 1^{-+} and 0^{++} states and their excited states, respectively. The leading order contribution to (4) including the quark and gluon condensate contributions has already been given in [11]

$$\Pi_v^0(q^2) = -\left[\frac{\alpha_s}{240\pi^3}(q^2)^3 + \frac{1}{36\pi}q^2(\langle\alpha_s G^2\rangle + 8\alpha_s\langle m\bar{u}u\rangle)\right]\ln(\frac{-q^2}{u^2}) \tag{5}$$
$$+ \left[\frac{4\pi}{9}\alpha_s\langle\bar{u}u\rangle^2 + \frac{1}{192\pi^2}g^3\langle G^3\rangle - \frac{83\alpha_s}{1728\pi}m\langle\bar{u}Gu\rangle\right],$$
$$\Pi_s^0(q^2) = \left[-\frac{\alpha_s}{480\pi^3}(q^2)^3 + (\frac{\alpha_s}{3\pi}\langle m\bar{u}u\rangle + \frac{\langle\alpha_s G^2\rangle}{24\pi})q^2 + \frac{m^2}{8\pi}\langle\alpha_s G^2\rangle + \frac{11\alpha_s}{72\pi}m\langle\bar{u}Gu\rangle\right]\ln(\frac{-q^2}{u^2})$$
$$+ 8\pi\alpha_s\langle\bar{u}u\rangle^2.$$

There is no difference for isovector and isoscalar currents in this order. The next-to-leading order correction to the perturbative part of $\Pi_v(q^2)$ and $\Pi_s(q^2)$ can be obtained by calculating the Feynman diagrams in Fig.2, where Figs.2m and 2n only contribute to the isoscalar states. The technique of the calculation which we use here was firstly proposed in [10].

Let us now briefly comment on the radiative corrections to the correlator of the current $g\bar{q}\gamma_5\gamma_\nu ig G_{\mu\nu}^a T^a q$ with 0^{--} and 1^{+-} quantum numbers. The isovector current correlator has the same radiative correction as the isovector current correlator of the $(0^{++}, 1^{-+})$ current. However, the isoscalar current correlator has different radiative corrections since diagrams Figs.2m and 2n, which correspond to the mixing with pure gluonic states, now give zero contributions.

Each of the diagrams Figs.2i-2n is gauge-parameter independent by itself because the current is antisymmetric in the Lorentz indices. We have checked on gauge invariance for the sum of diagrams Figs.2a-2h by doing the calculation in a general covariant gauge and found that the result is gauge-parameter independent. Explicit Feynman gauge results for the diagrams are listed in the appendix.

In the present application only the isovector currents are of interest. In the $\overline{\text{MS}}$-scheme, the next-to leading corrections to the correlator of isovector currents is given by

$$\Pi_v^{1a}(q^2) = -\frac{\alpha_s(\mu)}{240\pi^3}(q^2)^3 \ln(\frac{-q^2}{\mu^2}) \left[(\frac{53}{4} - \frac{76}{45}n_f)\frac{\alpha_s(\mu)}{\pi} - (\frac{35}{24} - \frac{1}{4}n_f)\frac{\alpha_s(\mu)}{\pi}\ln(\frac{-q^2}{\mu^2}) \right] \quad (6)$$

$$\Pi_s^{1a}(q^2) = -\frac{\alpha_s(\mu)}{480\pi^3}(q^2)^3 \ln(\frac{-q^2}{\mu^2}) \left[(\frac{2017}{216} - \frac{229}{180}n_f)\frac{\alpha_s(\mu)}{\pi} - (\frac{35}{24} - \frac{1}{4}n_f)\frac{\alpha_s(\mu)}{\pi}\ln(\frac{-q^2}{\mu^2}) \right]$$

where we take the light quark mass to be zero for convenience. Although (5) include condensates which are proportional to the light quark mass, their contributions are very small compared to those of operators with the same dimension. Throughout this calculation taking zero quark mass is a good approximation.

Eq.(6) does not contain the complete next-to leading order correction. one also has to include the contribution from the renormalization of the current. By inserting the renormalized currents (2) into the correlator

$$i \int d^4x e^{iqx} 2 Z_i^{\alpha_s} \langle 0|T\{j_\mu^1(x), j_\nu^{i+}(0)\}|0\rangle, \quad (7)$$

we obtain

$$\Pi_v^{1b}(q^2) = -\frac{\alpha_s(\mu)}{240\pi^3}(q^2)^3 \ln(\frac{-q^2}{\mu^2})((-\frac{91}{16} + \frac{39}{40}n_f)\frac{\alpha_s(\mu)}{\pi} + (\frac{35}{36} - \frac{1}{6}n_f)\frac{\alpha_s(\mu)}{\pi}\ln(\frac{-q^2}{\mu^2})) \quad (8)$$

$$\Pi_s^{1b}(q^2) = -\frac{\alpha_s(\mu)}{480\pi^3}(q^2)^3 \ln(\frac{-q^2}{\mu^2})((-\frac{679}{144} + \frac{97}{120}n_f)\frac{\alpha_s(\mu)}{\pi} + (\frac{35}{36} - \frac{1}{6}n_f)\frac{\alpha_s(\mu)}{\pi}\ln(\frac{-q^2}{\mu^2})).$$

In Eq.(7) we have introduced the notation $Z_1^{\alpha_s} = Z_1 Z_g - 1$ and $Z_i^{\alpha_s} = Z_i (i = 2, ..6)$. For the original hybrid current j_μ^1 one also has to include the counterterm Z_g resulting from the renormalization of the bare coupling constant g. The final result for the radiative corrections to the correlator is finally obtained by adding the contributions of (6) and (8).

4   Sum rules for 1^{-+} and 0^{++} hybrid mesons

For sum rule applications we need the spectral density associated with the current-current correlator. The spectral density $\rho_v(s) = Im\Pi_v(s)$ is defined via the standard dispersion relation

$$\Pi_v(q^2) = \frac{(q^2)^n}{\pi} \int_0^\infty ds \frac{\rho_v(s)}{s^n(s - q^2)} + \sum_{k=0}^{n-1} a_k(q^2)^k, \quad (9)$$

where the a_k are appropriate subtraction constants to render Eq.(9) finite.

From (5), (6) and (8) we obtain

$$\rho_v(s) = \frac{\alpha_s(\mu)}{240\pi^2}s^3(1 + \frac{1301}{240}\frac{\alpha_s(\mu)}{\pi} - \frac{17}{36}\frac{\alpha_s(\mu)}{\pi}\ln(\frac{s}{\mu^2})) + \frac{1}{36}s(\langle\alpha_s G^2\rangle + 8\alpha_s\langle m\bar{u}u\rangle) \quad (10)$$

$$\rho_s(s) = \frac{\alpha_s(\mu)}{480\pi^2}s^3(1 + \frac{6979}{2160}\frac{\alpha_s(\mu)}{\pi} - \frac{17}{36}\frac{\alpha_s(\mu)}{\pi}\ln(\frac{s}{\mu^2})) \quad (11)$$

$$-(\frac{\alpha_s}{3}\langle m\bar{u}u\rangle + \frac{\langle\alpha_s G^2\rangle}{24})s - \frac{m^2}{8}\langle\alpha_s G^2\rangle - \frac{11\alpha_s}{72}m\langle\bar{u}Gu\rangle,$$

where we have set $n_f = 3$.

On the other hand, the spectral density is saturated by narrow physical resonances and the continuum. We therefore write

$$(\frac{q_\mu q_\nu}{q^2} - g_{\mu\nu})\rho_v(s) = \sum_R \langle 0|j_\mu|R\rangle\langle R|j_\nu|0\rangle\pi\delta(s - m_R^2) + continuum, \quad (12)$$

where we have assumed that the mass m_R is much larger than the decay width of the hybrid, so that the imaginary part of the propagator has been replaced by $\pi\delta(s - m_R^2)$.

In order to extract information on the lowest-lying resonance, it is usually assumed that the lowest-lying resonance dominates the spectral density. The contribution of higher excited states can be suppressed by applying the Borel transformation $\hat{L}_M$ to both sides of Eq. (9). One thus has

$$R_0(\tau) = M\hat{L}_M\Pi_v(q^2) = \frac{1}{\pi}\int_0^\infty e^{-s/M}\rho_v(s)ds. \quad (13)$$

The upper limit of the intergral can be replaced by a finite number s_0. The contributions beyond the threshold s_0 are considered to result from the continuum. $R_0(\tau)$ is the zeroth moment. Higher order moments are defined by $R_k = (M^2\frac{\partial}{\partial M})^k R_0(M)$. Resonance masses can be obtained by taking the ratio $m_R^2 = \frac{R_{k+1}}{R_k}$ with the assumption that only a single narrow resonance dominates. In principle any value of k can be chosen to determine the resonance masses. However, since we have to truncate the series of the power expansion, using higher moments will damage the convergence of the OPE. Besides, it is also arbitrary to define the scalar function $\Pi_v^k(q^2) = \frac{1}{(q^2)^k}\Pi_v(q^2)$ by extracting a general tensor factor

$$(q^2)^k(\frac{q_\mu q_\nu}{q^2} - g_{\mu\nu}) \quad (14)$$

from the correlator (4). Although (13) can be considered as a higher moment of $\Pi_v^k(q^2)$, to the order of OPE that we are considering, the sum rules for $\Pi_v^k(q^2)$ and $\Pi_v(q^2)$ are obviously different. For instance, as pointed out in [11], the dimension-six operators of (5) do not contribute to sum rule (13), while they play an important role in stabilizing the sum rule of $\Pi_v^k(q^2)$ in the case of $k = 1$. We shall consider the two cases $k = 0$ and $k = 1$ in turn.

The single particle matrix elements contributing to (12) are parametrized as

$$\langle 0|j_\mu|V\rangle = i\epsilon_\mu f_v m_v^3. \quad (15)$$
$$\langle 0|j_\mu|S\rangle = ip_\mu f_s m_s^2.$$

In the narrow resonance approximation the sum rules are independent of the matrix element (15). When the decay width of the resonance is comparable with its mass, the approximation

5

(12) is no longer valid. Then the information contained in (15) may become important. We will comment on this later on. By using (10)-(15) we obtain

$$m_{v,s}^2 = \frac{\int_0^{s_0} e^{-s\tau} s\rho_{v,s}(s)ds}{\int_0^{s_0} e^{-s\tau} \rho_{v,s}(s)ds} \tag{16}$$

for the sum rule (13) and

$$m_v^2 = \frac{\int_0^{s_0} e^{-s\tau} \rho_v(s)ds}{\int_0^{s_0} e^{-s\tau} \rho_v(s)ds/s - \frac{4\pi^2}{9}\alpha_s\langle\bar{u}u\rangle^2 - \frac{1}{192\pi}g^3\langle G^2\rangle + \frac{83}{1728}\alpha_s m\langle\bar{u}Gu\rangle} \tag{17}$$

$$m_s^2 = \frac{\int_0^{s_0} e^{-s\tau} \rho_s(s)ds}{\int_0^{s_0} e^{-s\tau} \rho_s(s)ds/s - 8\pi^2\alpha_s\langle\bar{u}u\rangle^2}$$

for the sum rule for $\Pi_v^k(q^2)$ with $k = 1$, where the spectral densities $\rho_{v,s}(s)$ are given in (10). The various parameters entering in (16)-(17) are specified as [12]

$$\Lambda_{QCD} = 0.25 GeV, \qquad m = 0.01 GeV, \qquad m\langle\bar{u}u\rangle = -\frac{1}{4}f_\pi^2 m_\pi^2 \tag{18}$$

$$\langle\alpha_s G^2\rangle = 0.04 Gev^4, \quad g^3\langle G^3\rangle = 1.1 GeV^2\langle\alpha_s G^2\rangle, \quad f_\pi = 0.132 GeV$$

$$\alpha_s(\mu) = \frac{4\pi}{9\ln(\frac{\mu^2}{\Lambda_{QCD}^2})}, \qquad \mu = 2 GeV, \qquad g\langle\bar{u}Gu\rangle = 1.5 Gev^2\langle\bar{u}u\rangle$$

In Fig.3 and Fig.4 we show a mass plot of the 1^{-+} state in its dependence on the Borel parameter M in the two sum rule ratios. The second sum rule gives a smaller mass which we will take as the lower bound.

The sensitivity of the mass to the choice of the threshold value s_0 is obvious. The mass will go to infinity when both s_0 and M go to infinity, because, when M goes to infinity, the Borel measure (13) no longer suppresses the continuum. In order to give a reasonable estimate, we set s_0 around 4 GeV^2. Fig.5 shows that m_v takes values around 3 GeV when s_0 is set to infinity. In Fig.6 one cannot find any stable point in the two-dimensional (s_0,M) space. Therefore, before fixing s_0, we cannot make any precise prediction for the hybrid mass. However, if one believes that the 1^{-+} hybrid mass lies around 2 GeV, s_0 should be larger than 4 GeV^2. This results in a lower bound for the 1^{-+} mass of 1.55 GeV(see Fig.2). The radiative corrections enhance the lower bound which gives QCDSR less room to accommodate recent experimental data.

The prediction of the mass is also sensitive to the form of the spectral density. This is mostly due to a truncated OPE. The contributions from higher dimension operators are very likely not small. The uncertainty from the narrow resonance approximation in (12) does not seem to reduce this discrepancy. This can be checked by replacing the narrow resonance form $\pi\delta(s - m_R^2)$ in (12) by the Breit-Wigner form

$$\frac{\Gamma_R m_R}{(s - m_R^2)^2 + \Gamma^2 m_R^2}. \tag{19}$$

Γ_R is the width of the 1^{-+} hybrid. When we choose $\Gamma_R = 200 MeV$ and a parametrization of the matrix element (15) in the form $\langle 0|j_\mu|V\rangle = i\epsilon_\mu m_R \bar{f}_v s^x$ with $\bar{f}_v$ constant and $x = 0.5\div1.5$, the hybrid mass is not sensitive to using the full Breit-Wigner form propagator. We show

the change in the Figs.3 and 4 by dotted lines. The discrepancy between the two cases k=0 and k=1 is still big and the mass predictions become somewhat larger.

The sum rule for the 0^{++} hybrid is shown in Figs.7 and 8 for the two cases, k=0 and k=1 resp., where we set $s_0 = 7$ GeV^2. The radiative corrections reduce the discrepancy between the two cases. Similar to the 1^{-+} case, when s_0 goes to infinity, the prediction of mass is around 3 GeV. It means that the contribution of the continuum dominates over that of the resonances. Therefore, the value chosen for the threshold s_0 is important.

5   Summary

In summary, we have calculated the next-to-leading order corrections to the two point correlator of the current $g\bar{q}\gamma_\nu iG^a_{\mu\nu}T^a q(x)$. We recalculated the masses of the 1^{-+} and 0^{++} hybrids. We find that the radiative corrections reduce the lower bound of the 1^{-+} mass and leave less room for QCD sum rules to fit the recent experimental data.

Note added in proof: While preparing this paper for publication, we became aware of a recent paper by K. Chetyrkin and S. Narison which addresses similar problems[13].

References

[1] D. R. Thompson *et al.* (E852 Collab.), Phys. Rev. Lett. **79** (1997) 1630.

[2] A. Abele *et al.* (Crystal Barrel Collab.), Phys. Lett. B**423** (1998) 175.

[3] G.S. Adams *et al*(E852 Collab.), Phys. Rev. Lett. **81** (1998) 5760.

[4] F.E. Close and E.S. Swanson, Phys. Rev. **D52**(1995)5242.

[5] C. Michael, Proceedings of HADRON97; P. Lacock *et al* (UKQCDCollaboration), Phys. Lett.**B401**(1997)307; C. Bernard *et al.* (MILC Collaboration), Phys. Rev. **D56**(1997)7039; C. Morningstar, Proceedings of HADRON97.

[6] F. E. Close and P. R. Page, Nucl. Phys. **B443** (1995) 233.

[7] M. A. Shifman, A. I. Vainshtein and V. I. Zakharov, Nucl. Phys. B**147** (1979) 385.

[8] S.D. Joglekar and B.W. Lee, Ann. Phys. **97** (1976) 160; W.S. Deans and J.A. Dixon, Phys. Rev. **D18** (1978) 1113; C.T. Hill, Nucl. Phys. **B156** (1979) 417.

[9] S. Narison, hep-ph/9909470 and therein.

[10] K.G. Chetyrkin, F.V. Tkachev, Nucl. Phys. **B192**(1981)159.

[11] I.I. Balitsky, D.I. Diakonov, A.V. Yung, Phys. Lett.**B112**(1982)71.
I.I. Balitsky, D.I. Diakonov, A.V. Yung, Z. Phys. **C33**(1986)265.
J. Govaerts, F.de. Viron, D. Gushin and J. Weyers, Phys. Lett.**B128**(1984)262.
J. Govaerts, F.de. Viron, D. Gushin and J. Weyers, Nucl. phys.**B248**(1984)1.
J.I. Latorre, S. Narison and P. Pascual, Z.Phys.**C34**(1987)347.
J. Govaerts, L.J. Reinders, P. Franken, X. Gonze and J. Weyers, Nucl. Phys.**B284** (1987) 674.

[12] L.J. Reinders, H. Rubinstein, S. Yazaki, Phys. Rep. **127**(1985)1.

[13] K. Chetyrkin and S. Narison, hep-ph/0003151.

Appendix In this appendix we list the results of calculating the diagrams Fig.2 in the Feynman gauge for the correlator (4).

$$Fig.2a \quad : \quad C\left[(\frac{637}{3840} - \frac{3}{128}\ln(\frac{-q^2}{\mu^2}))g_{\mu\nu} + (-\frac{143}{640} + \frac{9}{256}\ln(\frac{-q^2}{\mu^2}))\frac{q_\mu q_\nu}{q^2}\right]$$

$$Fig.2b \quad : \quad C\left[(-\frac{673}{172800} + \frac{1}{1920}\ln(\frac{-q^2}{\mu^2}))g_{\mu\nu} + (\frac{9}{1600} - \frac{1}{1280}\ln(\frac{-q^2}{\mu^2}))\frac{q_\mu q_\nu}{q^2}\right]$$

$$Fig.2c \quad : \quad C\left[\frac{1}{480}g_{\mu\nu} + (-\frac{307}{3840} + \frac{3}{256}\ln(\frac{-q^2}{\mu^2}))\frac{q_\mu q_\nu}{q^2}\right]$$

$$Fig.2d \quad : \quad C\left[(-\frac{157}{1600} + \frac{9}{640}\ln(\frac{-q^2}{\mu^2}))g_{\mu\nu} + (\frac{867}{6400} - \frac{27}{1280}\ln(\frac{-q^2}{\mu^2}))\frac{q_\mu q_\nu}{q^2}\right]$$

$$Fig.2e \quad : \quad C\left[(-\frac{583}{21600} + \frac{1}{240}\ln(\frac{-q^2}{\mu^2}))g_{\mu\nu} + (\frac{31}{800} - \frac{1}{160}\ln(\frac{-q^2}{\mu^2}))\frac{q_\mu q_\nu}{q^2}\right]$$

$$Fig.2f \quad : \quad C\left[\frac{1}{640}g_{\mu\nu} + \frac{1}{640}\frac{q_\mu q_\nu}{q^2}\right]$$

$$Fig.2(g+h+i) \quad : \quad C\left[(\frac{79}{1440} - \frac{19}{2700}n_f - (\frac{1}{128} - \frac{1}{960}n_f)\ln(\frac{-q^2}{\mu^2}))g_{\mu\nu}\right.$$

$$\left. +(-\frac{97}{1280} + \frac{31}{3200}n_f + (\frac{3}{256} - \frac{1}{640}n_f)\ln(\frac{-q^2}{\mu^2}))\frac{q_\mu q_\nu}{q^2}\right]$$

$$Fig.2j \quad : \quad C\left[(-\frac{1}{24} + \frac{1}{144}\ln(\frac{-q^2}{\mu^2}))g_{\mu\nu} + (\frac{25}{216} - \frac{1}{48}\ln(\frac{-q^2}{\mu^2}))\frac{q_\mu q_\nu}{q^2}\right]$$

$$Fig.2k \quad : \quad C\left[-\frac{1}{720}g_{\mu\nu} + \frac{13}{3240}\frac{q_\mu q_\nu}{q^2}\right]$$

$$Fig.2l \quad : \quad C\left[(\frac{83}{28800} - \frac{1}{1920}\ln(\frac{-q^2}{\mu^2}))g_{\mu\nu} + (\frac{289}{86400} - \frac{1}{1920}\ln(\frac{-q^2}{\mu^2}))\frac{q_\mu q_\nu}{q^2}\right]$$

$$Fig.2m \quad : \quad C\left[-\frac{1}{8640}g_{\mu\nu} - \frac{1}{1440}\frac{q_\mu q_\nu}{q^2}\right]$$

$$Fig.2n \quad : \quad C\left[(\frac{71}{5400} - \frac{1}{480}\ln(\frac{-q^2}{\mu^2}))g_{\mu\nu} + (-\frac{401}{21600} + \frac{1}{320}\ln(\frac{-q^2}{\mu^2}))\frac{q_\mu q_\nu}{q^2}\right]$$

We use the abbreviation $C = \frac{\alpha_s(\mu)^2}{\pi^4}(q^2)^3\ln(\frac{-q^2}{\mu^2})$.

Figure captions

Fig. 1 Feynman diagrams for the renormalization of the hybrid current. Dots stand for the current vertices.

Fig. 2. Feynman diagrams for the next-to-leading calculation. Dots stand for the current vertices.

Fig. 3. 1^{-+} hybrid mass m_v versus Borel variable M for the first sum rule Eq.(16). Dashed line gives the result for the leading order calculation. Solid line includes radiative corrections. Dotted line gives the results when using the Breit-Wigner resonance propagator.

Fig. 4. 1^{-+} hybrid mass m_v versus Borel variable M for the second sum rule Eq.(17)

Fig. 5. 1^{-+} hybrid mass m_v versus Borel variable M for the second sum rule Eq.(17) when s_0 goes to infinity.

Fig. 6. Three-dimensional figure of 1^{-+} hybrid mass m_v vs. the Borel variable M and the threshold parameter s_0.

Fig. 7. 0^{++} hybrid mass m_s versus Borel variable M for the first sum rule Eq.(16). Solid line inculdes radiative corrections.

Fig. 8. 0^{++} hybrid mass m_s versus Borel variable M for the second sum rule Eq.(17). Solid line includes radiative correction.
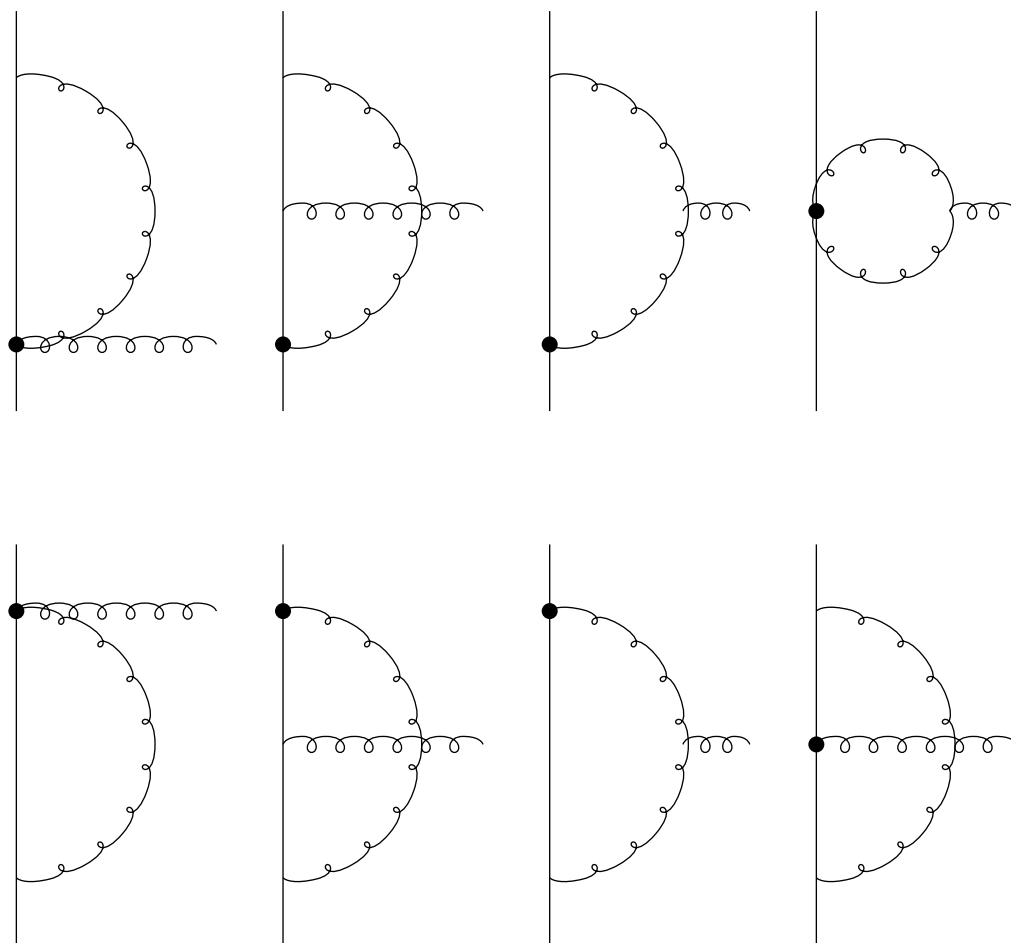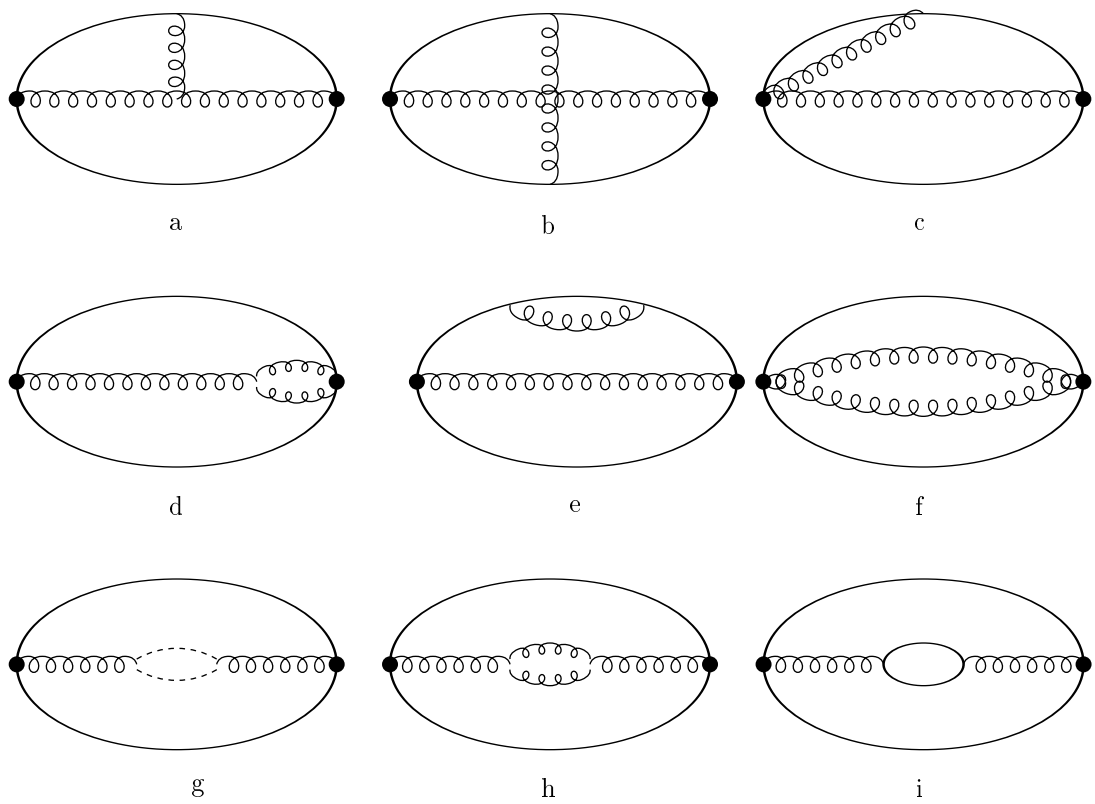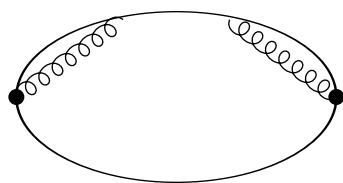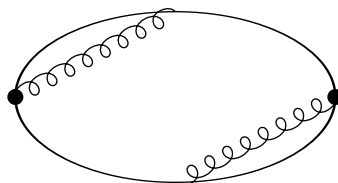
Fig.1

a

b

c

d

e

f

g

h

i

44

Fig.2

j

k

l

m

n

Fig.2